2006 ANNUAL REPORT

STRESS SPATIAL HETEROGENEITY AND ITS EFFECT ON EARTHQUAKE RUPTURE

Principal Investigator: Daniel Lavallée
Institution: Institute for Crustal Studies, University of California, Santa Barbara

The results related to this research project are reported in the following papers:

Lavallée, D., P. Liu, R. J. Archuleta, 2005. Stochastic model of heterogeneity in earthquake slip spatial distributions. *Geophys. J. Int.*, **165**, 622-640, 2006.

Lavallée, D. On the Random Nature of Earthquake Sources and Ground Motions: A Unified Theory. Submitted to *Scattering of Short-Period Seismic Waves in Earth Heterogeneity*, eds. H. Sato and M. Fehler. In review, 2007.

During the period going from 01/01/06 to 01/31/07, in addition to the 2006 annual meeting, I participated to three workshops sponsored by SCEC —the SCEC Broadband Ground Motion Simulation Workshop (May 22), the Broadband Strong Motion Simulation Platform (June 30), and the Broadband Strong Motion Simulation Platform Demonstration (Nov 2).

1 Numerical Simulations Earthquake Rupture Propagation Under Heterogeneous Conditions

In this research project, we consider a simple configuration for the fault model based on the fault model used in "SCEC 3D Rupture dynamics, Validation of the Numerical Simulation Method" (Harris *et al.*, 2005). The following settings are adopted for the faults. We consider a rectangular vertical fault of 30 km by 15 km. A square nucleation patch (or asperity) is located in the center of the fault with dimension of 3 km by 3 km. In the nucleation patch, the initial shear stress is along the strike direction and is set to 81.6 MPa. The nucleation point is at the center of the square nucleation patch. Except for the initial shear stress, all the other parameters used in these simulations such as the initial yield stress and the parameters of a linear slip-weakening friction law (Ida, 1972), are uniform across the fault surface. The parameters are listed in Harris *et al.*, (2005). The initial shear stress along the dip direction is set to 0 everywhere on the fault surface. The material properties of the medium surrounding the fault are given by $v_p = 6000$ m/sec, $v_s = 3464$ m/sec and the density is 2670 kg/m^3. The basic idea with these simulations is to capture and isolate the effect of the shear stress variability on the rupture.

Except for the square nucleation patch described above, the initial shear stress along the strike direction is spatially heterogeneous. We used a random model to describe the shear stress heterogeneity. A random model is specified by a set of random variables and by the rules used to transform the random variables. Here we consider two situations: the random variables are distributed over a two-dimensional grid according to a Gauss law (see Liu-Zeng *et al.*, 2005) or according to Cauchy law (see Lavallée and Archuleta, 2003: Lavallée *et al.*, 2006; and Liu *et al.* 2006). The rules are essentially given by a generalization of the fractional Brownian motion to Cauchy (or more generally Lévy) random variables. It consists in a filtering in the two-dimensional Fourier space of the Fourier transform of the random variables by a function given by $k^{-\eta_{2D}}$ where $k = |\mathbf{k}|$ is the 2D radial wavelength number. We consider four values for the parameters η_{2D}: 0, 1/2, 1 and 2. The values 0, 1 and 2 are based on model of slip distributions with a Fourier amplitude characterized by an exponent $\eta_{2D} + 1 = 1$ (Lomnitz-Adler and Lemus-Diaz, 1989), $\eta_{2D} + 1 = 2$

(Herrero and Bernard, 1994) and $\eta_{2D}+1=3$ (Hanks, 1979) – see also Figure 3 of Herrero and Bernard (1994). Note that $\eta_{2d}=0$ corresponds to white noise and no filtering is needed.

The following procedure is devised to generate the shear stress spatial heterogeneity with a given value η_{2D}. Gauss random variables are generated using $\mu_{Gauss}=0$ and $\sigma_{Gauss}=1$. The random model is computed according to the procedure discussed above (for details see Lavallée *et al.*, 2006). The random model is normalized by the maximum value to obtain a distribution of values that varies approximately from −1 to +1. Adding 7 to the normalized random model and multiplying the resulting field by 10^7 give the random shear stress spatial distribution. Due to these normalizations, the random shear stress spatial distribution ranges approximately between 60 and 80 MPa. The maximum value doesn't exceed the shear stress value of 81.6 MPa. A similar procedure is used to generate Cauchy random variables (with $\mu_{Cauchy}=0$ and $\gamma_{Cauchy}=1$) with an additional constraint. The range of the Cauchy random variables has to be limited between a minimum value and a maximum value. (This problem can be ignored for Gauss random variables since the probability to generate extremely large values is very small and in practice can be ignored.) Although we compute scenarios of rupture for different set of values of minimum and maximum (-10 to 10, -15 to 15, -20 to 20 and -25 to 25) we only discussed the results obtained for a range of random variables that goes from -15 to 15. Then the same filtering and normalization are performed to obtain the random shear stress.

It should be noted that random shear stress generated according to this procedure is also distributed according to a Gauss (or Cauchy) law, but with the parameters μ_{Gauss} (or μ_{Cauchy}) and σ_{Gauss} (or γ_{Cauchy}) function of the position on the fault (for details see Lavallée, 2007). Note also that scenarios of shear stress based on Gauss random variables have the same range of values than those of the scenarios of shear stress based on Cauchy random variables. However, frequency of large (or small) fluctuation from the "average" of 70 MPa is significantly more important for shear stress distributed according to a Cauchy law. This difference seems to affect the propagation of the rupture.

Using the model discussed above, we developed eight banks of scenarios of shear stress heterogeneity. They are divided into two groups. The first group includes four banks based on the same Gauss parameters, and the second group includes four banks based on the Cauchy parameters. Within each group, the four banks of scenario only differ by the value of the parameter η_{2D}. We used a 3D finite element (FE) codes developed by S. Ma (Ma, 2006), to simulate the rupture initiation and the propagation of the rupture under heterogeneous conditions. Snapshots of the dynamic rupture process are illustrated in Figure 1.

An additional complication when computing scenarios of rupture under heterogeneous conditions is the interruption of the rupture process before the rupture front reaches the fault limits. It is certainly not obvious that each statistically similar slip distribution will lead to a dynamic rupture that sweeps over the entire fault. (Some additional criteria may have to be found to solve this problem–see Vidal *et al.* 2000). This behavior is a consequence of the spatial variability in the shear stress. However the interruption is not systematic and our results suggest a dependence on the degree of correlations of the shear stress controlled by the parameter η_{2D}.

When the parameter $\eta_{2D}=0$ or ½, fluctuations in shear stress are spatially punctual ($\eta_{2D}=0$) or located over patch areas of small dimensions ($\eta_{2D}=1/2$). The surface dimension of the patches is not large enough to affect the propagation of the rupture fronts. For all the scenarios of rupture computed with the Gauss law and the Cauchy law, the rupture spreads over the fault surface. The presence of the shear stress heterogeneity essentially produces deformations of a rather smooth rupture front (See Figure 2).

When the parameter $\eta_{2D} = 1$, some irregular patterns of larger dimension appeared in the shear stress spatial distribution. These patterns have two main consequences. The first is the interruption of the rupture process when the rupture front leaves the central nucleation patch. These interruptions are observed for 30% of the Gauss scenarios and 20% of the Cauchy scenarios. For 10% of the Gauss scenarios and 10% of the Cauchy scenarios the rupture covers between 50% and 90% of the fault before before stopping. Finally for 70% of the Gauss scenarios and 60% of the Cauchy scenarios the rupture process covers more than 90% of the fault area. Deformations of the rupture front are significantly more important for scenarios generated with $\eta_{2D} = 1$ (see Figure 2).

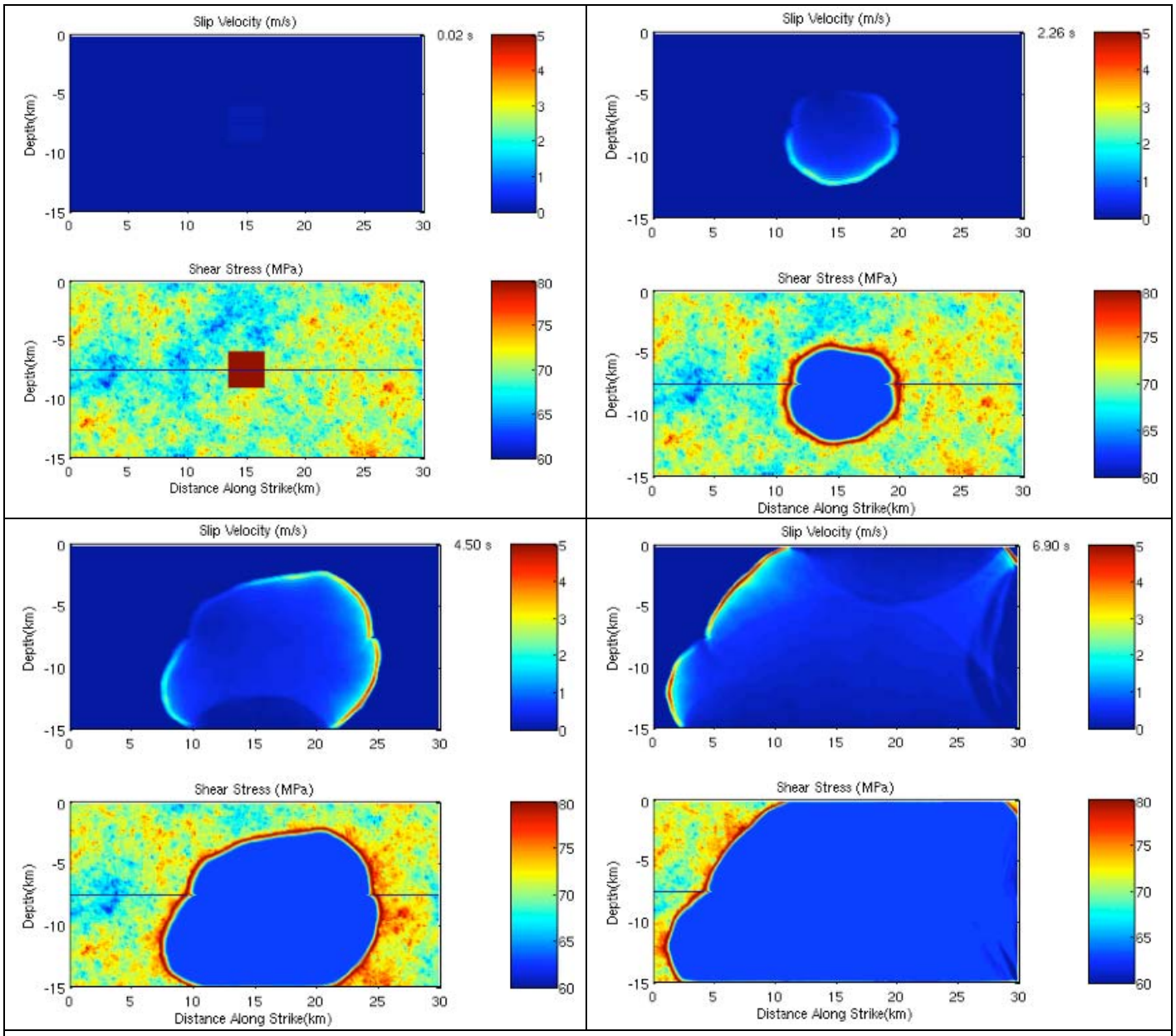

Figure 1: Snapshots of the simulations of the dynamic rupture model in a homogeneous elastic medium at different time interval for a Cauchy scenario with $\eta_{2D} = 1$. The slip velocity and the shear stress are illustrated. Rupture starts from a finite initial asperity and initially grows in all direction. After the initial phase, the propagation of the rupture front is gradually becoming asymmetrical with respect to the initial square nucleation patch. This behavior is typical of simulations with $\eta_{2D} = 1$ and $\eta_{2D} = 2$.

Finally when $\eta_{2D} = 2$, irregular patterns of large dimensions characterized the shear stress spatial distribution. The presence of large fluctuating spatial patterns of high and shear stress accentuates the behavior reported for the scenarios computed with $\eta_{2D} = 1$. There is a larger number of interruptions after the rupture front leaves the central nucleation patch. Such interruptions are observed for 40% of the Gauss scenarios and 30% of the Cauchy scenarios. For 40% of the Gauss scenarios and 50% of the Cauchy scenarios the rupture process covers between 50% and 90% of the fault area. Finally, for 20% of the Gauss scenarios and 20% of the Cauchy scenarios the rupture process covers more than 90% of the fault surface. For $\eta_{2D} = 2$, the rupture front time evolution is more complicated as suggested by the curves of the rupture front in Figure 2.

2 Discussion

According to these results, the degree of correlation in the initial shear stress, controlled by the η_{2D}, constrained the propagation of the rupture fronts. The behavior is reminiscent of percolation theory, except that in percolation theory, observation of percolation is related to connecting the two opposites of the system under consideration by one unbroken chain of nearest neighbors (see Stauffer and Aharony, 1994). This is usually done by investigating the distribution of values in the system under consideration, i.e., the one-point statistic. However the percolation is not conditional to the degree of correlation characterizing the system under consideration.

Through the disorder that characterizes earthquake spatial distribution, many authors have identified the importance of spatial pattern. For instance, and to keep it with stress spatial variability, it has been argued that the presence of patches with high stress values is essential for rupture to expand. Assuming different planar fault geometry, Andrews (1976) and Day (1982) have computed the critical lengths characterizing the size of the minimum patches. Introducing the effect of lubrification in fault mechanics, Brodsky and Kanamori (2001) note that many discontinuous lubricated regions are required at the surface of the fault in order to observe slipping. In numerical modeling the 1994 Northridge, California, earthquake, Nielsen and Olsen (1999) not only concur that high stress patches on the fault are needed for rupture to process, but they also introduce the idea that connectivity between the patches is also essential for the progression of the rupture front. According to Madariaga and Olsen (2002), rupture propagation is controlled by a non-dimensional parameter (corresponding approximately to the ratio of the available strain energy to the energy release rate). Rupture propagation is conditional to exceeding a critical value of the non-dimensional parameter. Interruption of the rupture process for heterogeneous distribution of stress has also been reported in the Peyrat *et al*. 2001. The results obtained in our study suggest that the factor impeding or limiting the rupture process is the degree of correlation (or two-points statistic) characterizing the initial shear stress.

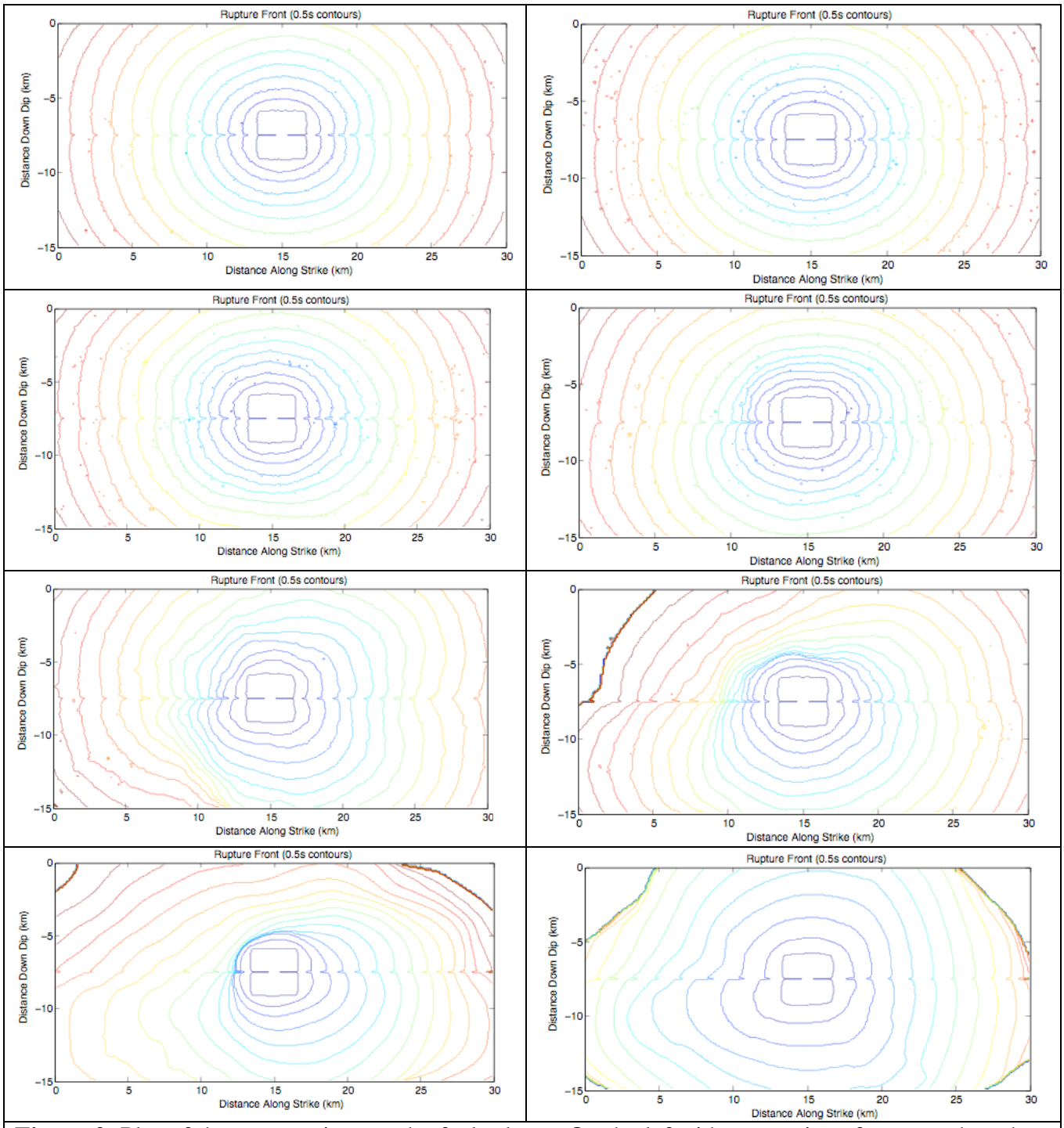

Figure 2: Plot of the rupture time on the fault plane. On the left side, scenarios of ruptures based on Gauss random variables. On the right side scenarios of ruptures based on Cauchy random variables. From top to bottom the parameter η_{2D} takes values 0, ½, 1 and 2.

References

Andrews, D. J. Rupture Velocity of Plane Strain Shear Cracks. *J. Geophys. Res.*, **81**, 5679-5687, 1976.

Brodsky, E. E., and H. Kanamori. Elastohydrodynamic lubrification of faults. *J. Geophys. Res.*, **106**, 16,357-16,374, 2001.

Day, S. M. Three-dimensional Simulation of Spontaneous Rupture. The effect of Non-uniform Prestress. *Bull. Seismol. Soc. Am.*, **72**, 1881-1902, 1982.

Hanks, T. C., *b* values and ω^{γ} seismic source models: implications for tectonic stress variation along active crustal faults zones and estimation of high-frequency strong ground motion, *J. Geophys. Res.*, *84*, 2235-2242, 1979.

Harris, R., R. Archuleta, B. Aagaard, J. P. Ampuero, D. J. Andrews, J, Bielak, S. Day, E. Dunham, N. Lapusta, D. Oglesby, K. Olsen, A. Pitarka, and J. Rice. 3D Rupture Dynamics, Validation of the Numerical Simulation Method. @005 SCEC Progress Report. 23 pp, 2005.

Herrero, A. and P. Bernard. A kinematic self-similar rupture process for earthquake. *Bull. Seism. Soc. Am.*, **84**, 1216-1228, 1994.

Ida, Y. Cohesive force across the tip of a longitudinal-shear crack and Griffith's specific surface energy, *J. Geophys. Res.*, **77**, 3796–3805, 1972.

Lavallée, D. On the Random Nature of Earthquake Sources and Ground Motions: A Unified Theory. Submitted to *Scattering of Short-Period Seismic Waves in Earth Heterogeneity*, eds. H. Sato and M. Fehler. In review, 2007.

Lavallée, D., P. Liu, R. J. Archuleta, 2005. Stochastic model of heterogeneity in earthquake slip spatial distributions. *Geophys. J. Int.*, **165**, 622-640, 2006.

Lavallée, D. and R. J. Archuleta. Stochastic modeling of slip spatial complexities for the 1979 Imperial Valley, California, earthquake. *Geophys. Res. Lett.*, **30** (5), 1245, doi:10.1029/2002GL015839, 2003.

Liu, P., R. Archuleta, and S. Hartzell. Prediction of Broadband Ground-Motion Time Histories: Hybrid Low/High-Frequency Method with Correlated Random Source Parameters. *Bull. Seism. Soc.*, 96 (6), doi:10.1785/0120060036. To be printed December, 2006.

Liu-Zeng, J., T. Heaton, and C. DiCaprio, The effect of slip variability on earthquake slip-length scaling. . *Geophys. J. Int.*, **162** (3), doi: 10.1111/j.1365-246X.2005.02679.x. 841-849, 2005.

Lomnitz-Adler, J. and P. Lemus-Diaz. A stochastic model for fracture growth on a heterogeneous seismic fault. *Geophys. J. Int.*, **99**, 183-194, 1989.

Ma, S. Using the Dynamics of Faulting to Explore Radiated Seismic Energy and Ground Motion. PhD dissertation. 207pp.

Madariaga, R., and K. B. Olsen. Criticality of rupture dynamics in 3-D. *Pure appl. Geophys.*, **157**, 1981-2001, 2002.

Nielsen, S. B. and K. B. Olsen. Models of the 1994 Nothridge, California, earthquake: dynamical constrains on stress and friction. *Pure appl. Geophys.*, **157**, ,1999.

Peyrat, S., K. Olsen, and R. Madariaga. Dynamic modeling of the 1992 Landers earthquake. *J. Geophys. Res.*, **106**, 26,467-236,482, 2001.

Stauffer, D., and A. Aharony. Introduction to percolation theory. Taylor & Francis Ltd., London. 181pp., 1994.

Vidal, V., D. Lavallée, and R. J. Archuleta.. Study of Heterogeneous Spatial Stress and Slip Distribution Along the Fault Surface. Supplement to EOS, Transactions, AGU, **81**, n0. 48, F865, 2000.